Service Duration Maximization for Continuous Coverage in UAV-Assisted Communication System

Jyotirindra Dandapat, Nishant Gupta, *Student Member, IEEE*, Satyam Agarwal, *Member, IEEE*, and Sam Darshi, *Senior Member, IEEE*

***Abstract*— This letter studies a UAV-assisted communication design where a rotary-wing UAV is launched to provide continuous coverage to mobile nodes. We aim to maximize the service time duration of the UAV by optimizing its three-dimensional (3D) trajectory while simultaneously ensuring adequate coverage to mobile nodes. Considering the limited energy available with the UAV, we frame an equivalent energy consumption minimization problem. Though the formulated problem is non-convex, it is shown that it is pseudoconvex under horizontal and vertical UAV coordinates. Based on this observation, we use alternating optimization to solve the problem. Numerical results provide trajectory insight and compare the service duration to the mobile nodes with different schemes.**

***Index Terms*— UAV communication, energy consumption, outage minimization, mobile nodes, trajectory design.**

I. Introduction

UNMANNED aerial vehicles (UAVs), owing to their high mobility and on-demand deployment, have gained much attention to assist the wireless communication system. In particular, they are mostly deployed as aerial base station (ABS) to provide enhanced service to the mobile ground nodes. For instance, in rescue missions, fire-fighters or users in a procession [1]. In general, the nodes are mobile and as the node location changes, the links between the UAV and the node also varies significantly affecting the communication performance. Therefore, the main requirement for a robust communication system is its ability to serve mobile nodes reliably and provide continuous network coverage over a longer time frame.

Furthermore, UAVs have limited onboard energy. The time frame for which the UAV can provide continuous coverage to the mobile ground node is limited and it majorly depends upon the UAV's trajectory. Therefore, UAV's limited energy leads to service discontinuity. In this letter, a UAV-assisted communication system is studied where a rotary-wing UAV serves the mobile ground nodes. This has gained recent attention in applications where the mobile node needs special coverage for a longer time durations. This includes scenario like search, and rescue and military operations where the UAV has to track the ground nodes to maintain continuous coverage for longer durations. To maximize the service time duration of the UAV-assisted communication system, we minimize the energy consumption of the UAV in manoeuvring while ensuring continuous coverage to the mobile ground nodes.

In the existing literature, the works that considered the UAV as ABS to serve the ground nodes consider the nodes to be static [2]. In reality, the UAV needs to track the location of the mobile node and develop a trajectory based on the node's location to enhance the communication performance. Towards this end, in [3], the authors studied an optimal UAV deployment system considering the moving node with the minimum quality-of-service (QoS) requirement for each node. In [4], the authors considered the node mobility to minimize the UAV transmit power while satisfying the node minimum rate requirements. However, they do not consider the energy consumption of the UAV. The authors in [5] optimized the two-dimensional (2D) trajectory and resource of the UAV to minimize the average computation energy of the ground node while considering the UAV energy consumption. The authors in [6] have also considered the user-centric objective that minimizes the maximum energy consumption over all nodes by optimizing the trajectory and task data allocation. The authors in [7] maximized the energy efficiency of a UAV but hadn't taken into account the probabilistic line-of-sight (LoS) channel model and assumed the UAV to fly at a constant altitude. A similar formulation has also been considered in [8] but for a fixed-wing UAV. The UAV limited energy constraint to maximize the service time duration in a dynamic environment while considering a practical probabilistic LoS and fading channel model has not been considered in the existing literature.

In this letter, a UAV-assisted communication system is studied to design the UAV trajectory considering the mobile nodes. The key contributions of this letter are listed as follows:

- We develop a framework to maximize the service time duration provided by the UAV to the mobile nodes by optimizing the UAV trajectory while ensuring continuous network coverage to the mobile nodes.
- To achieve this, we formulate an equivalent problem that minimizes the energy consumed by the UAV in each time slot.
- Noting the non-convexity, we propose an iterative approach based on alternating optimization to obtain a sub-optimal three-dimensional (3D) UAV trajectory.
- Finally, we evaluate the performance of the proposed scheme. In particular, using our proposed approach, the approximate time served by the UAV is increased by 25%.

This work applies to many practical applications, such as providing coverage to mobile ground nodes in a procession or first responders in case of an emergency. In such applications,

Manuscript received 27 May 2022; revised 2 July 2022; accepted 5 July 2022. Date of publication 11 July 2022; date of current version 10 October 2022. This work was supported in part by the Department of Science and Technology under Grant DST/INSPIRE/04/2016/001127, CRG/2020/005749 and in part by IIT Ropar ISIRD Grant under Grant 9-362/2018/IITRPR/1590. The associate editor coordinating the review of this letter and approving it for publication was H. Ghazzai. *(Corresponding author: Nishant Gupta.)*

The authors are with the Department of Electrical Engineering, Indian Institute of Technology (IIT) Ropar, Ropar 140001, India (e-mail: 2020eem1008@iitrpr.ac.in; 2018eez0018@iitrpr.ac.in; satyam@iitrpr.ac.in; sam@iitrpr.ac.in).

Digital Object Identifier 10.1109/LCOMM.2022.3189692

the UAV needs to track the node's movements to provide continuous coverage for maximum time duration.

II. System Model

We consider a wireless communication system where a rotary-wing UAV is launched from the location $(\mathrm{x}_0^u, \mathrm{y}_0^u, \mathrm{z}_0^u)$ and acts as an ABS to provide coverage to K ground nodes labelled as $\mathcal{K} \triangleq \{1, \cdots, K\}$ using frequency division multiple access (FDMA) scheme. Through FDMA, we assume that the equal channel bandwidth is allocated to each node by the serving UAV. This avoids interference between different links and maintains fairness among mobile nodes. For simplicity, time is slotted with slot duration equal to τ, where τ is set to be sufficiently small [9]. Then, the location of the UAV at the n^{th}-time slot in 3D-Cartesian coordinate is represented as $(x^u[n], y^u[n], z^u[n])$. Furthermore, we assume the UAV flies with velocity $v^u[n]$ which is decomposed into its horizontal component $v_{xy}^u[n] = [v_x^u[n], v_y^u[n]]$ and vertical component $v_z^u[n]$.

We assume K ground nodes moving independently in a 2D rectangular field. We assume that the node location is known to the UAV but only at the beginning of every time slot. This can be achieved by employing tracking algorithms [10], [11]. Location of the k^{th}-node at the n^{th}-time slot is given as $[x_k[n], y_k[n]], \forall k \in \mathcal{K}$. Accordingly, the distance between the UAV and the k^{th}-node at any time slot n is given by $d_k[n] = \sqrt{(x^u[n] - x_k[n])^2 + (y^u[n] - y_k[n])^2 + z^u[n]^2}$.

We consider a realistic channel model between the UAV and the ground mobile nodes that is modelled by both the large-scale attenuation $l_k[n]$ and the small-scale fading $h_k[n]$. Furthermore, the receiver is assumed to perfectly compensate for the Doppler effect caused by UAV mobility based on existing techniques [12]. The large-scale attenuation is modelled separately for LoS and NLoS links defined as $l_k^{LoS}[n] = \beta_0 d_k[n]^{-\bar{\alpha}}$ and $l_k^{NLoS}[n] = \kappa\beta_0 d_k[n]^{-\bar{\alpha}}$, respectively. Here $\bar{\alpha}$, κ, $d_k[n]$ and d_0 represent the pathloss exponent, additional attenuation coefficient due to NLoS link, distance between the UAV and the k^{th}-node, and reference distance, respectively. The probability of having a LoS link between the k^{th}-node and the UAV at the n^{th}-time slot is a function of elevation angle [4] which is given by

$$P_{LoS} = (1 + b_1 \exp(-b_2[\phi_k[n] - b_1]))^{-1}, \tag{1}$$

where $\phi_k[n] = \frac{180}{\pi} \sin^{-1}\left(\frac{z^u[n]}{d_k[n]}\right)$ is the elevation angle of the UAV with the k^{th}-node and b_1, and b_2 correspond to the nature of environment such as, urban, sub-urban, etc. Then, the average channel power gain $l_k[n]$ is modelled as [1]

$$l_k[n] = P_{LoS} d_0 d_k[n]^{-\bar{\alpha}} + (1 - P_{LoS})\kappa d_0 d_k[n]^{-\bar{\alpha}}. \tag{2}$$

We assume the small-scale fading channel coefficient $h_k[n]$ follows Nakagami-m distribution with $\mathbb{E}[|h_k[n]|^2] = 1$. Because the channel is modelled for both LoS and NLoS links, the Nakagami-m distribution is adopted as it can model both types of channel while maintaining analytical tractability. Then, the received signal-to-noise ratio (SNR) at the k^{th}-node is given by $\gamma_k[n] = \frac{P_{tr} l_k[n] |h_k[n]|^2}{\sigma^2}$, where P_{tr} and σ^2 is the transmit power and noise power, respectively. For a Nakagami-m distributed random variable $h_k[n]$, $|h_k[n]|^2$ follows Gamma distribution. Then, the cumulative density function (CDF) of SNR $\gamma_k[n]$ follows Gamma distribution which is given by [13]

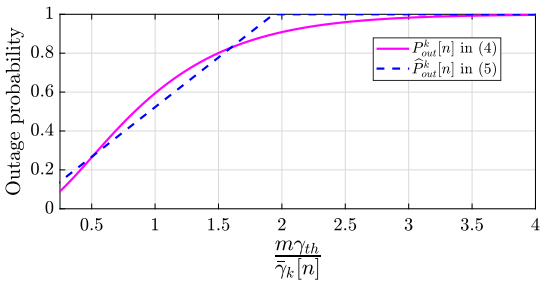

Fig. 1. Outage probability of exact and approximated expression for different $\frac{m\gamma_{th}}{\bar{\gamma}_k[n]}$.

$$F_{\gamma_k[n]}(\gamma) = 1 - \frac{1}{\Gamma(m)}\Gamma\left(m, \frac{m}{\bar{\gamma}_k[n]}\gamma\right), \tag{3}$$

where $\bar{\gamma}_k[n] = \frac{P_{tr} l_k[n]}{\sigma^2}$ and $\Gamma(.)$ is the gamma function.

To define the coverage metric, we consider the outage probability as the performance metric. Outage probability is defined as the probability that the received SNR of the mobile node falls below the required threshold γ_{th}. Then, the outage probability is given as follows

$$P_{out}^k[n] = Pr(\gamma_k[n] < \gamma_{th}) = F_{\gamma_k[n]}(\gamma_{th}), \tag{4}$$

where the CDF of $F_{\gamma_k[n]}(\gamma_k[n])$ is defined in (3). It is highly complicated to compute the outage probability defined in (4). Thus, we utilize the curve fitting approach to fit $P_{out}^k[n]$ for simplification. Towards this end, the polynomial curve fitting approach approximates $P_{out}^k[n]$ to

$$\widehat{P}_{out}^k[n] = a_1 + a_2 m \frac{\gamma_{th}}{\bar{\gamma}_k[n]}, \tag{5}$$

where a_1, a_2 are the curve fitting parameters.

Remark 1: The curve fitting is chosen to approximate the outage probability defined in (4) such that the error is minimized. The approximation error c_ϵ is defined as $c_\epsilon = |P_{out}^k[n] - \widehat{P}_{out}^k[n]|/P_{out}^k[n]$, where $|.|$ is the absolute value. Furthermore, we compute the coefficient of determination (R-squared) that assesses the correlation between two functions, it is also referred to as "*goodness of fit*", and is represented by a value ranging from 0 to 1. Value 1 indicates a perfect fit while value 0 indicates worst fit. For the sample values $a_1 = 0.0545$, and $a_2 = 0.4610$, the correlation between the approximation and exact is 97% ($\mathrm{R}^2 = 0.97$). Fig. 1 shows the variation in outage probability for $P_{out}^k[n]$ in (4) and $\widehat{P}_{out}^k[n]$ in (5) for different $\frac{m\gamma_{th}}{\bar{\gamma}_k[n]}$.

The power consumption of the rotary-wing UAV comprises of propulsion power that depends upon UAV manoeuvring. Then, the overall energy consumed by the UAV in the n^{th}-time slot is given by [14]

$$\begin{aligned} e[n] = \tau P_0 &\left(1 + \frac{v_{xy}^u[n]^2}{U_{tip}^2}\right) \\ &+ \tau P_i \left(\sqrt{1 + \frac{v_{xy}^u[n]^4}{4v_0^4}} - \frac{v_{xy}^u[n]^2}{2v_0^2}\right)^{\frac{1}{2}} \\ &+ \frac{\tau d_f \rho s A_r v_{xy}^u[n]^3}{2} + \tau W v_z^u[n], \end{aligned} \tag{6}$$

where $P_0, P_i, U_{tip}, d_f, \rho, s, A_r$, and W are the constants as described in Section V.

III. Problem Formulation

In this letter, our objective is to maximize the service time of the UAV by optimizing the UAV trajectory while simultaneously ensuring that the ground nodes always remain in coverage. Since time is discretized into time slots of equal duration, then maximizing the service duration is equivalent to maximizing the number of time slots. The optimization problem is formulated as

$$\begin{aligned} \text{P1}: \quad & \max_{\mathcal{T}\triangleq\{(x^u[n],y^u[n],z^u[n]),\forall n\in\{1,\cdots,N\}\}} \quad N \\ & \text{s.t.}: \ (C1): \widehat{P}^k_{out}[n] \leq P^{th}_{out}, \\ & \qquad \forall k \in \mathcal{K}, \quad \forall n \in \{1,\cdots,N\}, \\ & \qquad (C2): \sum_{n=1}^{N} e[n] \leq E_{max}, \end{aligned}$$

where $(C1)$ is the coverage constraint with P^{th}_{out} being the threshold outage probability, $(C2)$ is the total energy consumption constraint with E_{max} being the maximum energy available with the UAV and $\mathcal{T} \triangleq \{x^u[n], y^u[n], z^u[n], \forall n \in \{1,\cdots,N\}\}$ is the trajectory of the UAV. The objective N represents the number of time slots for which the UAV will provide communication to the ground nodes. Therefore, N is an integer variable. Since the constraints in P1 are also dependent on N, the problem P1 is non-convex and NP-hard. To handle the tractability of problem P1, we introduce the following property to make an equivalent problem of P1.

Property 1: Since the time for which the UAV provides coverage to the ground nodes relies on the energy available with the UAV, maximizing the number of time slots can be alternatively interpreted as minimizing the energy consumed by the UAV in each time slot.

Hence, the solution to problem P1 can be equivalently obtained from the following algorithm in each time slot.

1: $N \leftarrow 1$
2: **while** $\sum_{n=1}^{N} e[n] \leq E_{max}$ **do**
3: $\quad \text{P2}[n]: \min_{x^u[n],y^u[n],z^u[n]} \quad e[n]$
$\qquad \text{s.t.:} \quad \text{(C3)}: \widehat{P}^k_{out}[n] \leq P^{th}_{out}, \quad \forall k \in \mathcal{K}$
4: $\quad N \leftarrow N + 1$

In each time slot, we are minimizing the energy consumed until the total energy is exhausted. The problem P2$[n]$ is a n^{th}-time slot problem that aims to minimize the energy consumed in that particular time slot. Thus, to maximize N, the problem P2$[n]$ is solved repeatedly until constraint $(C2)$ is violated. Problem P2$[n]$ is still a non-convex optimization problem due to the presence of the non-convex objective and constraint. To solve this problem, we present an iterative approach using alternating optimization in the following section.

IV. Proposed Methodology

In this section, before providing the solution approach, we first describe the analytical insights of the objective and the constraints using the following lemmas.

Lemma 1: $\widehat{P}^k_{out}$ defined in $(C3)$ is a jointly pseudoconvex function of x^u and y^u for any given value of z^u, and $\widehat{P}^k_{out}$ is a pseudoconvex function of z^u for any given value of x^u and y^u.

Proof: See Appendix. ∎

Lemma 2: The energy consumed by the UAV is a pseudoconvex and linear function with respect to $x^u[n]$ and $y^u[n]$, and $z^u[n]$, respectively.

Algorithm 1 Alternating Optimization to Solve P2$[n]$

Require: $(x_k, y_k), \forall k \in \mathcal{K}$, and ϵ.
Ensure: $\mathcal{X}^* = (x^u[n]^*, y^u[n]^*, z^u[n]^*), \forall n \in \{1,\cdots,N^*\}$.
1: Initialize $r = 1$.
2: **repeat**
3: Solve P2$[n]$ for fixed $z^u[n]_r$ to obtain $x^u[n]^*_{r+1}$ and $y^u[n]^*_{r+1}$.
4: Solve P2$[n]$ for fixed $x^u[n]^*_{r+1}$ and $y^u[n]^*_{r+1}$ to obtain $z^u[n]^*_{r+1}$.
5: Compute $e[n]_{r+1}$ from $(x^u[n]^*_{r+1}, y^u[n]^*_{r+1}, z^u[n]^*_{r+1})$.
6: Set $r = r + 1$.
7: **Until** $|e[n]_{r+1} - e[n]_r| \leq \epsilon$
8: $(x^u[n]^*, y^u[n]^*, z^u[n]^*) = (x^u[n]_{r+1}, y^u[n]_{r+1}, z^u[n]_{r+1})$ and $e[n]^* = e[n]_{r+1}$.

Proof: This result can be easily proved by using Lemma 1 in [9]. ∎

Accounting above lemmas, it can be observed that since the objective and constraint function are pseudoconvex function jointly in $(x^u[n], y^u[n])$, and individually in $z^u[n]$, therefore, the problem P2$[n]$ is a pseudoconvex problem. Thus, a low-complexity alternating minimization approach is employed to obtain a sub-optimal solution of P2$[n]$. In alternating minimization, at each iteration r, the algorithm first obtains optimal $x^u[n]^*_{r+1}$ and $y^u[n]^*_{r+1}$ for fixed $z^u[n]$ and using the obtained $x^u[n]^*_{r+1}$ and $y^u[n]^*_{r+1}$, it obtains $z^u[n]^*_{r+1}$. Note that since P2$[n]$ is pseudoconvex in $(x^u[n], y^u[n])$, and $z^u[n]$, the interior point method can be effectively used to obtain the optimal values. At each iteration r, it computes the energy consumed by the UAV in a time slot denoted by $e[n]_{r+1}$. The alternating algorithm stops when $|e[n]_{r+1} - e[n]_r| \leq \epsilon$, where $e[n]_{r+1}$ and $e[n]_r$ is the energy consumed per time slot at the $(r+1)^{th}$ and r^{th}-iteration, respectively, and ϵ is the predefined acceptable tolerance. The overall algorithm to obtain the solution of P2$[n]$ is described in Algorithm 1. This alternating approach is repeated with an update in the time slot index, node's and UAV current location until $\sum_{n=1}^{N} e[n] < E_{max}$. Finally the algorithm returns the $e[n]^*$ and the optimal UAV locations $(x^u[n]^*, y^u[n]^*, z^u[n]^*), \forall n$.

V. Simulation Results

In this section, we provide numerical and graphical results to validate our proposed scheme. In our setup, the UAV initial location is set to $(0, 0, 15)$ m with $E_{max} = 1400$ J. The channel parameters are taken as $\tilde{\gamma}_0 = 52.5$ dB, $\gamma_{th} = -3.01$ dB, $b_1 = 10$, $b_2 = 0.6$, $\kappa = 0.2$, and $\bar{\alpha} = 2.3$ [9]. The outage probability threshold P^{th}_{out} as defined in $(C3)$ is set to 0.1. The problem is solved using alternating optimization with ϵ set to 10^{-6}. The time slot duration is set to 0.1 s. The values taken for energy consumption model are as follows: $P_o = 79.86$ W represents the blade profile power, $P_i = 88.63$ W represents the induced power; $W = 20$ N, $A_r = 0.503$, $U_{tip} = 120$, $v_o = 4.03$ m/s, $d_f = 0.6$, $s = 0.05$, $\rho = 1.225$ are the aircraft's weight, rotor disc area, tip speed of rotor blade, induced velocity of rotor, fuselag drag ratio, rotor solidity and air density, respectively [1].

We consider three sample scenarios as shown in Fig. 2. For each scenario, we present the UAV trajectory, velocity, energy consumption per slot, cumulative energy consumption and outage probability in Fig. 2. The description for each scenario is as follows.

Scenario 1: A single node is considered moving with velocity 15 m/s in a single direction. It can be observed that

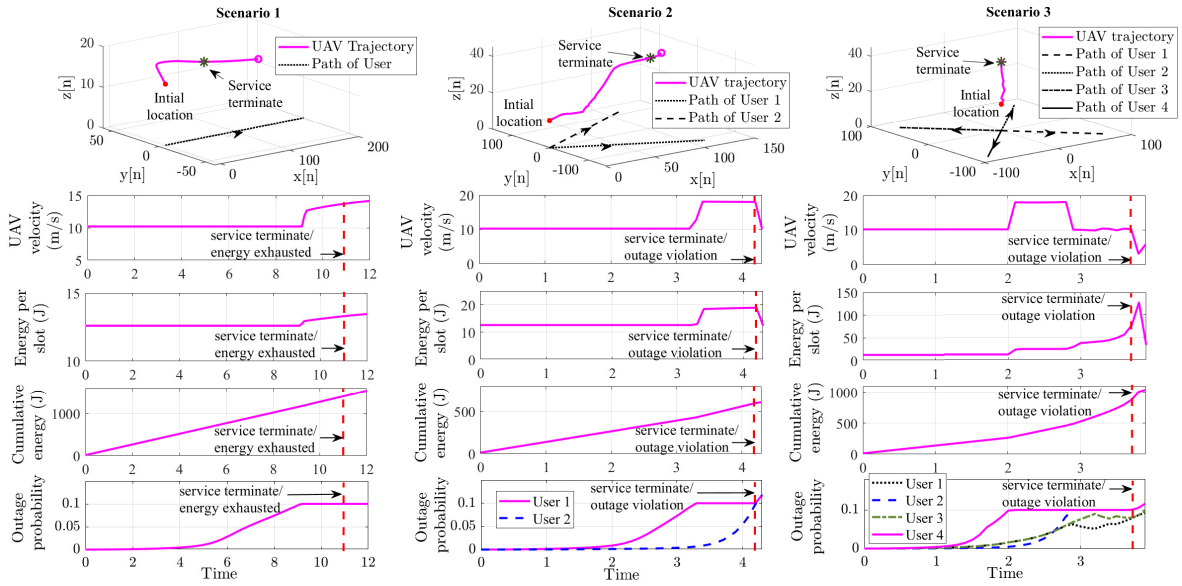

Fig. 2. UAV trajectory, velocity, energy consumption per slot, cumulative energy consumption and outage probability at each time slot.

UAV moves with the optimal velocity to minimize the onboard energy. As the node velocity is higher than the optimal UAV velocity, the outage probability increases with time. Later, when the outage probability approaches the given threshold P_{out}^{th}, the UAV moves with a higher velocity to track the node and meet the outage threshold P_{out}^{th}. In this case, UAV will provide service till its available energy is exhausted.

Scenario 2: Two nodes moving with velocity 15 m/s starting from the same location and moving ninety degrees apart as shown in Fig. 2. It can be observed that to maintain an appropriate coverage between the two nodes, the UAV moves in horizontal direction with lesser velocity and later increases its velocity. But as the nodes are going farther from the UAV, to maintain the outage probability, the UAV moves in both the horizontal and vertical direction with a higher velocity. In this case, after certain time, when the nodes are far apart that they cannot be served, outage exceeds the threshold. At this point the UAV service terminates.

Scenario 3: Four nodes moving opposite to each other with velocity 15 m/s as shown in Fig. 2. It can be observed that as the nodes are going opposite to each other, the UAV first travels in horizontal direction to minimize the energy and later moves in the vertical direction to reduce the outage probability. This is because the UAV consumes lesser energy while travelling in horizontal direction than in the vertical direction. However, similar to Scenario 2, after certain time the UAV is unable to meet the outage threshold P_{out}^{th} as the nodes are far apart. At this point the service terminates.

To show the performance comparison of our proposed scheme, we consider three benchmark schemes, namely centroid-based trajectory [15], strip-based trajectory [16], and travelling salesman problem (TSP)-based trajectory [17] as shown in Fig. 3. In centroid-based trajectory, the UAV moves to the centroid of all users at each time slot; a strip-based trajectory traces a strip pattern in a rectangular field with fixed velocity. In a TSP-based trajectory, the sequence of nodes to be visited is first computed while minimizing the energy consumption of the UAV, and then the UAV's next location is

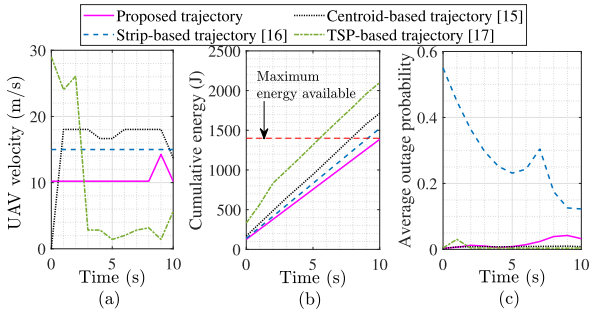

Fig. 3. Comparison of (a) UAV velocity, (b) cumulative energy, and (c) average outage probability of proposed scheme with the benchmark schemes.

set to the next node's location to be visited. In these schemes, the UAV is assumed to fly at a fixed altitude.

For this result, we consider 10 nodes following a random waypoint method to travel within a rectangular 100×100 m^2 area [3]. It can be observed that the proposed scheme consumes lesser energy compared to the other schemes and thus with a given onboard energy, it can serve the ground nodes for a longer time. Furthermore, it can be observed that the outage probability of the centroid-based and TSP-based trajectory is quite less than the proposed scheme, but the energy consumption corresponding to their trajectory is quite high. Since our objective is to maximize the service duration, the proposed scheme extends the service duration and obtains an optimal UAV trajectory while maintaining the outage probability of each node within the required threshold P_{out}^{th}. This threshold ensures that the UAV provides sufficient coverage to the ground nodes. In general, after evaluating the proposed approach for 100 random scenarios where the movement of node follows random waypoint method, the approximate time served by the UAV increased by 25% as compared to the benchmark schemes.

VI. Conclusion

In this letter, we provide a new framework where a UAV optimizes the 3D trajectory to provide continuous coverage to the mobile ground nodes. In particular, we maximize the

service time duration by minimizing the energy consumed by the UAV in each time slot until the available energy is exhausted. Based on the alternating optimization approach, we provide a sub-optimal solution to the optimization problem. Simulation results shows the effectiveness of the proposed scheme in terms of lesser energy consumption and higher service time. Future extensions include mobile node prediction in future times and UAV trajectory design under noise environment.

APPENDIX
INDIVIDUAL PSEUDOCONVEXITY OF $\widehat{P}^k_{out}$ IN (x^u, y^u) FOR FIXED z^u AND IN z^u FOR FIXED (x^u, y^u)

We will omit $[n]$ throughout this proof. From (5), since a_1 is constant, we consider only the third term $\bar{P}^k_{out} = a_2 m \frac{\gamma_{th}}{\tilde{\gamma}_k}$ to prove the pseudoconvexity of (5). Considering $\rho_k = \sqrt{(x^u - x_k)^2 + (y^u - y_k)^2}, \forall k \in \mathcal{K}$, where ρ_k represents the horizontal distance between the projection of UAV on the ground and the k^{th}-node. It can also be written in the form of $\rho_k = \sqrt{f(x^u, y^u)}$, where $f(x^u, y^u) = (x^u - x_k)^2 + (y^u - y_k)^2$. The function $f(x^u, y^u)$ has $\frac{\partial^2 f(x^u, y^u)}{\partial (x^u)^2} = 2$, $\frac{\partial^2 f(x^u, y^u)}{\partial (y^u)^2} = 2$, and $\frac{\partial^2 f(x^u, y^u)}{\partial y^u \partial x^u} = \frac{\partial^2 f(x^u, y^u)}{\partial x^u \partial y^u} = 0$, then, $det[\mathcal{H}(f(x^u, y^u))] > 0$, where Hessian $\mathcal{H}(f(x^u, y^u)) = \begin{bmatrix} \frac{\partial^2 f(x^u, y^u)}{\partial (x^u)^2} & \frac{\partial^2 f(x^u, y^u)}{\partial x^u \partial y^u} \\ \frac{\partial^2 f(x^u, y^u)}{\partial y^u \partial x^u} & \frac{\partial^2 f(x^u, y^u)}{\partial (y^u)^2} \end{bmatrix}$. This implies that $f(x^u, y^u)$ is jointly convex in x^u and y^u. Since square root is a monotonic increasing function, therefore it preserves the convexity [18]. Substituting ρ_k in $\bar{P}^k_{out}$, we get,

$$\bar{P}^k_{out} \triangleq \frac{\frac{\gamma_{th}}{\tilde{\gamma}_o}(\rho_k^2 + (z^u)^2)^{\alpha}}{\frac{(1-\kappa)}{1+b_1 \exp\left(-b_2\left[\frac{180}{\pi}\sin^{-1}\left(\frac{(z^u)}{\sqrt{(\rho_k^2+(z^u)^2)}}\right)-b_1\right]\right)} + \kappa}, \quad (7)$$

where $\tilde{\gamma}_o = \frac{P_{tx} d_0}{a_2 m \sigma^2}$. Since ρ_k is jointly convex in x^u and y^u, then proving convexity of $\bar{P}^k_{out}$ defined in (7) with respect to ρ_k will result in joint convexity of $\bar{P}^k_{out}$ in x^u and y^u.

The double derivative of $\bar{P}^k_{out}$ with respect to ρ_k is given as

$$\frac{\partial^2 \bar{P}^k_{out}}{\partial \rho_k^2} = \mathcal{A}\left[\frac{w_k b_2 z^u}{\alpha\pi}\left(\frac{(2\alpha-1)\rho_k}{(w_k\kappa+1)^2} + \frac{90 b_2 z^u (1-w_k\kappa)}{\pi(w_k\kappa+1)^3}\right) + \frac{(w_k+1)\left((2\alpha-1)\rho_k^2 + (z^u)^2\right)}{180(1-\kappa)(w_k\kappa+1)}\right], \quad (8)$$

where $\mathcal{A} = 360\alpha\frac{\gamma_{th}}{\tilde{\gamma}_o}(1-\kappa)\left(\rho_k^2 + (z^u)^2\right)^{\alpha-2}$ and $w_k = b_1 \exp\left(-b_2\left(\frac{180}{\pi}\sin^{-1}\left(\frac{z^u}{\sqrt{\rho_k^2+(z^u)^2}}\right) - b_1\right)\right)$. It is observed that, $\frac{\partial^2 \bar{P}^k_{out}}{\partial \rho_k^2}$ is positive for all values of ρ_k when z^u is fixed. This implies the convexity of $\bar{P}^k_{out}$ in ρ_k. As a result, $\bar{P}^k_{out}$ is jointly convex (also psuedoconvex) in x^u and y^u for fixed z^u [19].

To show the pseudoconvexity of $\bar{P}^k_{out}$ with z^u for fixed x^u and y^u, let $z_0 \triangleq \left\{ z^u \middle| \left(\frac{\partial \bar{P}^k_{out}}{\partial z^u} = \mathcal{G}_1 - \mathcal{G}_2 = 0 \right) \right\}$, where

$$\mathcal{G}_1 \triangleq 2\alpha \frac{\gamma_{th}}{\tilde{\gamma}_o} z^u \frac{(1+w_k)\mathcal{A}_k}{1+w_k\kappa}, \quad (9)$$

$$\mathcal{G}_2 \triangleq 180 \frac{\gamma_{th}}{\tilde{\gamma}_o} \frac{b_2 w_k (1-\kappa)\mathcal{A}_k \sqrt{(x^u - x_k)^2 + (y^u - y_k)^2}}{\pi(1+\kappa w_k)^2}, \quad (10)$$

$\mathcal{A}_k = \left[(x^u - x_k)^2 + (y^u - y_k)^2 + (z^u)^2\right]^{\alpha-1}$ and $w_k = b_1 \exp\left(-b_2\left(\frac{180}{\pi}\sin^{-1}\left(\frac{z^u}{\sqrt{(x^u-x_k)^2+(y^u-y_k)^2+(z^u)^2}}\right) - b_1\right)\right)$. Using (9) and (10), we observe that $\mathcal{G}_1 > \mathcal{G}_2$ for $z^u > z_0$ and $\mathcal{G}_1 < \mathcal{G}_2$, otherwise. This implies $\frac{\partial \bar{P}^k_{out}}{\partial z^u} > 0$ *i.e.,* increasing function for $z^u > z_0$ and $\frac{\partial \bar{P}^k_{out}}{\partial z^u} < 0$, *i.e.,* decreasing function for $z^u < z_0$. This proves the pseudoconvexity of $\bar{P}^k_{out}$ with respect to z^u for a given x^u and y^u.

REFERENCES

[1] Y. Zeng, J. Xu, and R. Zhang, "Energy minimization for wireless communication with rotary-wing UAV," *IEEE Trans. Wireless Commun.*, vol. 18, no. 4, pp. 2329–2345, Apr. 2019.

[2] M. Alzenad, A. El-Keyi, F. Lagum, and H. Yanikomeroglu, "3-D placement of an unmanned aerial vehicle base station (UAV-BS) for energy-efficient maximal coverage," *IEEE Wireless Commun. Lett.*, vol. 6, no. 4, pp. 434–437, Aug. 2017.

[3] R. Ghanavi, E. Kalantari, M. Sabbaghian, H. Yanikomeroglu, and A. Yongacoglu, "Efficient 3D aerial base station placement considering users mobility by reinforcement learning," in *Proc. IEEE Wireless Commun. Netw. Conf. (WCNC)*, Barcelona, Spain, Apr. 2018, pp. 1–6.

[4] A. H. Sawalmeh, N. S. Othman, H. Shakhatreh, and A. Khreishah, "Wireless coverage for mobile users in dynamic environments using UAV," *IEEE Access*, vol. 7, pp. 126376–126390, 2019.

[5] Z. Yang, S. Bi, and Y.-J. A. Zhang, "Dynamic trajectory and offloading control of UAV-enabled MEC under user mobility," in *Proc. IEEE Int. Conf. Commun. Workshops (ICC Workshops)*, Montreal, QC, Canada, Jun. 2021, pp. 1–6.

[6] X. Diao, J. Zheng, Y. Cai, Y. Wu, and A. Anpalagan, "Fair data allocation and trajectory optimization for UAV-assisted mobile edge computing," *IEEE Commun. Lett.*, vol. 23, no. 12, pp. 2357–2361, Dec. 2019.

[7] Z. Liu *et al.*, "UAV-aided vehicular communication design with vehicle trajectory's prediction," *IEEE Wireless Commun. Lett.*, vol. 10, no. 6, pp. 1212–1216, Jun. 2021.

[8] S. Eom, H. Lee, J. Park, and I. Lee, "UAV-aided wireless communication designs with propulsion energy limitations," *IEEE Trans. Veh. Technol.*, vol. 69, no. 1, pp. 651–662, Jan. 2020.

[9] N. Gupta, D. Mishra, and S. Agarwal, "Energy-aware trajectory design for outage minimization in UAV-assisted communication systems," *IEEE Trans. Green Commun. Netw.*, early access, Jan. 26, 2022, doi: 10.1109/TGCN.2022.3146627.

[10] H. Sallouha, M. M. Azari, A. Chiumento, and S. Pollin, "Aerial anchors positioning for reliable RSS-based outdoor localization in urban environments," *IEEE Wireless Commun. Lett.*, vol. 7, no. 3, pp. 376–379, Jun. 2018.

[11] G. Han, J. Jiang, C. Zhang, T. Q. Duong, M. Guizani, and G. K. Karagiannidis, "A survey on mobile anchor node assisted localization in wireless sensor networks," *IEEE Commun. Surveys Tuts.*, vol. 18, no. 3, pp. 2220–2243, Mar. 2016.

[12] U. Mengali, *Synchronization Techniques for Digital Receivers*. New York, NY, USA: Springer, Nov. 2013.

[13] A. Girdher, A. Bansal, and A. Dubey, "On the performance of SLIPT-enabled DF relay-aided hybrid OW/RF network," *IEEE Syst. J.*, early access, Jan. 4, 2022, doi: 10.1109/JSYST.2021.3135957.

[14] T. Zhang, G. Liu, H. Zhang, W. Kang, G. K. Karagiannidis, and A. Nallanathan, "Energy-efficient resource allocation and trajectory design for UAV relaying systems," *IEEE Trans. Commun.*, vol. 68, no. 10, pp. 6483–6498, Oct. 2020.

[15] Q. Wu, Y. Zeng, and R. Zhang, "Joint trajectory and communication design for multi-UAV enabled wireless networks," *IEEE Trans. Wireless Commun.*, vol. 17, no. 3, pp. 2109–2121, Mar. 2018.

[16] C. Zhan, Y. Zeng, and R. Zhang, "Trajectory design for distributed estimation in UAV-enabled wireless sensor network," *IEEE Trans. Veh. Techn.*, vol. 67, no. 10, pp. 10155–10159, Oct. 2018.

[17] J. Zhang, Y. Zeng, and R. Zhang, "UAV-enabled radio access network: Multi-mode communication and trajectory design," *IEEE Trans. Signal Process.*, vol. 66, no. 20, pp. 5269–5284, Oct. 2018.

[18] S. Boyd and L. Vandenberghe, *Convex Optimization*. Cambridge, U.K.: Cambridge Univ. Press, 2004.

[19] M. S. Bazaraa, H. D. Sherali, and C. M. Shetty, *Nonlinear Programming: Theory and Algorithms*. Hoboken, NJ, USA: Wiley, 2013.